

Heterocyclic compounds as acidizing corrosion inhibitors for carbon steel in acid media



Thesis submitted in partial fulfillment for the Award of
Degree

Doctor of Philosophy

By

Mohammad Salman

DEPARTMENT OF CHEMISTRY INDIAN
INSTITUTE OF TECHNOLOGY (BANARAS HINDU
UNIVERSITY) VARANASI – 221005
INDIA


Roll No. 17051501

Year of Submission 2022

CERTIFICATE

It is certified that the work contained in the thesis titled “*Heterocyclic compounds as acidizing corrosion inhibitors for carbon steel in acid media*” by “*Mohammad Salman*” has been carried out under my supervision and that this work has not been submitted elsewhere for a degree.

It is further certified that the student has fulfilled all the requirements of Comprehensive Examination, Candidacy, and SOTA for the award of Ph.D. Degree.



Prof. Vandana Srivastava

(Supervisor)

Department of Chemistry
Indian Institute of Technology
(Banaras Hindu University)

Varanasi - 221005

Dr. Vandana Srivastava
Professor
Department of Chemistry
Indian Institute of Technology (BHU)
Varanasi-221005

DECLARATION BY CANDIDATES

I, "**Mohammad Salman**" certify that the work embodied in this thesis is my own bonafide work and carried out by me under the supervision of "**Prof.Vandana Srivastava**" from "**December 2017**" to "**2022**" at the "**Departement of Chemistry,**" **Indian Institute od Technology, Banaras Hindu University, varanasi.** The matter embodied in this thesis has not been submitted for the award of any other degree/diploma. I declare that I have faithfullyt acknowledged and given credits to the research workers wherever their works have been cited in my work in this thesis. I further declare that I have not willfully copied any others work, Paragraphs, text, data, results, etc., reported in journals, books, magazines, reports, dissertations, thesis etc., or available at websites and have not included them in this thesis and have not cited as my own work.

Date : 12/12/2022

Place : Varanasi

Mohd. Salman
Signature of the Student

("Mr. Mohammad Salman")

CERTIFICATE BY THE SUPERVISOR(S)

It is certified that the above statement made by the student is correct to the best of my knowledge.

Vandana
Prof. Vandana Srivatsva
(Supervisor)
Department of Chemistry
Indian Institute of Technology
Banaras Hindu University
Dr. Vandana Srivastava
Professor
Department of Chemistry
Indian Institute of Technology (BHU)
Varanasi-221005

Y.C. Sharma
Prof. Y.C. Sharma
Head of
Department of Chemistry
Indian Institute of Technology
Banaras Hindu University

COPYRIGHT TRANSFER CERTIFICATE

Title of the Thesis: *"Heterocyclic compounds as acidizing corrosion inhibitors for carbon steel in acid media"*

Name of the Student: *Mohammad Salman*

COPYRIGHT TRANSFER

The undersigned here by assigns to the Indian Institute of Technology (Banaras Hindu University) Varanasi all rights under copyright that may exist in and for the above thesis submitted for the award of the "*Doctor of Philosophy.*"

Date: *12/12/2022*

Mohd. Salman
Signature of the Student

Place: Varanasi

(Mr. Mohammad Salman)

Note: However, the author may reproduce or authorize others to reproduce material extracted verbatim from the thesis or derivative of the thesis for author's personal use provided that the source and the Institute's copyright notice are indicated.

ACKNOWLEDGEMENT

Firstly, I would like to express my sincere gratitude to my supervisor, Prof Vandana Srivastava, for the supervision, guidance and patience throughout my PhD research work.

I am also very grateful to Prof. M. A. Quraishi, Former Professor of the Department of Chemistry, Indian Institute of Technology, Banaras Hindu University, Varanasi (INDIA) and, Chair Professor at King Fahd University of Petroleum & Minerals, Dhahran, Saudi Arabia for invaluable discussions and important contributions to this work. I also thank him for introducing me to corrosion science and providing me many opportunities which are very important to my scientific career.

I am thankful to Prof. Y.C. Sharma, Head of the Department and former Heads of the Department of Chemistry Prof D. Tiwari and Prof R.B. Rastogi, Indian Institute of Technology, Banaras Hindu University, Varanasi, for providing necessary lab facilities and a congenial working atmosphere in the Department.

I would also like to thank my RPEC members, Prof. Rajiv Prakash and Dr. Akhilesh Kumar Singh (External Subject Expert), School of Material Science and technology, Indian Institute of Technology, Banaras Hindu University, Varanasi and Dr. Sundaram Singh (Internal Subject Expert), Department of Chemistry, Indian Institute of Technology, Banaras Hindu University, Varanasi, for their valuable suggestions throughout this work.

I gratefully acknowledge the facilities provided by the Centre of instrumental Facility, Indian Institute of technology, Banaras Hindu University, Varanasi.

I have a deep sense of gratitude for all Professors of the Department of Chemistry, Indian Institute of technology, Banaras Hindu University, Varanasi for their cooperation and inspiration.

I am thankful to non-teaching staff of the Department of Chemistry, Indian Institute of Technology, Banaras Hindu University, Varanasi, for their support. I am also thankful to the MHRD for providing financial assistance during my research work.

I am obliged to all my seniors, labmates and friends; Dr. Dheeraj Singh Chauhan, Dr. Chandrabhan Verma, Dr. Kashif Rahmani Ansari, Dr. Jiyaul Haque, Dr. Ankush Kumar Mishra, Dr. Pratibha Verma, Dr Swati Chauhan, Vishal Singh, Khushbu Rajput, Priya Mahaur and Md. Javed for their vital contributions in my research work.

I would like to acknowledge my indebtedness to my loving parents Mr. Moharram Ali & Mrs. Jaibunnisha and my family members' for their love, affection, prayers and support.

(Mohammad Salman)

(Research Scholar)

TABLE OF CONTENT

Chapter 1: Introduction	1-42
1.1 Definition of Corrosion	2
1.2 Economic losses	3
1.2.1 Direct losses	3
1.2.2 Indirect losses	3
1.3 General idea of Corrosion	4
1.3.1 Corrosion problems in oil/petroleum industry	5
1.3.2 Acidizing treatment in oil wells	5
1.3.3 Pickling	6
1.4 Classification of Corrosion	7
1.4.1 Chemical Corrosion or Dry Corrosion	7
1.4.2 Electrochemical Corrosion or Wet Corrosion	8
1.5 Different forms of corrosion	10
1.5.1 Uniform corrosion	11
1.5.2 Galvanic or two metal corrosion	12
1.5.3 Crevice Corrosion	12
1.5.4 Pitting Corrosion	13
1.5.5 Selective leaching or selective dissolution	14
1.5.6 Intergranular Corrosion	15
1.5.7 Stress-corrosion cracking	16
1.5.8 Erosion Corrosion	17
1.5.9 Hydrogen Damage	17
1.6 Factors Affecting Corrosion rate	18
1.6.1 Primary factors, depending on the metal	18
1.6.1.1 Nature of the metal	18
1.6.1.2 Surface state of the metal	18
1.6.1.3 Nature of the corrosion product	18
1.6.1.4 Hydrogen over voltage	19
1.6.2 Secondary factors related to the environment	19
1.6.2.1 pH of the medium	19

1.6.2.2 Temperature	19
1.6.2.3 Presence of oxidizing agents	20
1.6.2.4 Humidity	20
1.6.2.5 Presence of impurities in the atmosphere	20
1.6.2.6 Conductance of the medium	20
1.6.2.7 Area effect	21
1.6.2.8 Polarization at anodic and cathodic area	21
1.6.3 Electrochemical Theory of Corrosion	21
1.7 Thermodynamic Principles of Corrosion	24
1.7.1 Kinetics of Corrosion	25
1.7.2 Activation controlled corrosion	25
1.7.3 Diffusion controlled reaction	28
1.7.4 Diagrams associated to Kinetic parameters	29
1.7.4.1 Evans Diagram	29
1.7.5 Mixed Potential Theory	31
1.7.6 Tafel Extrapolation Method	33
1.7.7 Linear Polarization Resistance	34
1.7.8 Electrochemical Impedance Spectroscopy	35
1.7.9 Methods of Corrosion Control	38
1.7.9.1 Surface modification of metal and their alloys	38
1.7.9.2 Cathodic protection	39
1.7.9.3 Anodic protection	40
1.7.10 Other measures	41
1.7.10.1 Design	41
1.7.10.2 Electroplating	41
1.7.10.3 Metallic coatings	41
1.7.10.4 Organic coatings	41
Chapter 2: Literature review	
2.1 Corrosion Inhibitors	43
2.1.1 Definition of Inhibition	43

2.1.2 Definition of Inhibitor	43
2.1.3 Classification based on the effect on partial electrochemical reactions	44
2.1.3.1 Anodic inhibitors	45
2.1.3.2 Cathodic inhibitors	45
2.1.3.3 Mixed inhibitors	46
2.1.3.3.1 Inorganic inhibitors	47
2.1.3.3.2 Organic inhibitors	48
2.1.4 Classification based on reaction mechanism	48
2.1.4.1 Inhibition by adsorption	49
2.1.4.2 Inhibition by passivation	49
2.1.4.3 Inhibition by film formation	50
2.1.5 Interface inhibitors (Vapour phase)	50
2.2.1 Quantum chemical calculations in corrosion inhibition studies	51
2.3 Hetero-Cyclic Compounds as Corrosion Inhibitors	52
2.3.1 Triazine -based inhibitors	58
2.3.2 Naphthyridne based inhibitors	62
2.3.3 Quinolines based derivatives	64
2.3.4 Imidazole based inhibitors	66
2.4 The scope and importance of corrosion inhibitor technology	69
2.5 Objective of present study	69
Chapter 3: Materials and Methods	71-97
3.1 Materials	71
3.1.1 Chemicals used	71
3.1.2 Composition of Testing Material	71
3.1.3 Test specimen for electrochemical study	72
3.1.4 Test solutions	72
3.1.5 Inhibitors used	72
3.1.5.1. Synthesis of Substituted Triazines	75
3.1.5.2. Synthesis of Chromeno naphthyridines	79
3.1.5.3. Synthesis of Hydroxyquinoline derivatives	83
3.1.5.4 Synthesis of substituted benzimidazole	85

3.2 Equipment and Techniques Used	86
3.2.1. Characterization of the synthesized compounds	86
3.2.1.1 Determination of melting point	86
3.2.1.2 Determination of Corrosion Rate and Other related parameters	87
3.2.2 Electrochemical studies	88
3.2.2.1 Electrochemical impedance spectroscopy	89
3.2.2.2 Potentiodynamic Polarization Technique	90
3.2.3 Determination of Thermodynamics of Parameters	92
3.2.3.1 (i) Determination of Activation Energy	92
3.2.3.2 (ii) Determination of Enthalpy and Entropy of activation	93
3.2.3.3 (iii) Determination of Free Energy of Adsorption	93
3.2.3.4 (iv) Determination of Enthalpy and Entropy of Adsorption	94
3.2.4 Surface study	94
3.2.4.1 Scanning Electron Microscopy (SEM) study	94
3.2.4.2 Energy dispersive X-ray Spectroscopy (EDX) study	94
3.2.5 Theoretical study	95
3.2.5.1 Quantum chemical calculations	95
3.2.5.2 Molecular dynamics simulation	96
Chapter 4: Results and Discussion	98-202
4.1 Heterocyclic substituted Triazine as corrosion steel for carbon(N-80) steel	98
4.1.1 Wt loss measurements	99
4.1.1.1 Effect of inhibitor concentration	99
4.1.1.2 Adsorption isotherm	100
4.1.2 Electrochemical studies	103
4.1.2.1 Electrochemical Impedance Spectroscopy	103
4.1.2.2 Potentiodynamic polarization study	108
4.1.3 Surface study	111
4.1.3.1 UV-visible spectroscopy	111
4.1.3.2 FTIR spectral analysis	113
4.1.3.3 Atomic force microscopy (AFM) characterization	114
4.1.4 Mechanism of inhibition	116

4.1.5 Conclusions	117
4.2 Chromeno naphthyridines based heterocyclic compounds as novel acidizing corrosion inhibitors	118
4.2.1 Weight loss measurements	120
4.2.1.1 Effect of concentration	120
4.2.1.2 Adsorption studies	121
4.2.2 Electrochemical studies	122
4.2.2.1 Electrochemical impedance spectroscopy	122
4.2.2.2 Potentiodynamic polarization	128
4.2.3 Surface studies	131
4.2.3.1 Atomic force microscopy (AFM)	131
4.2.3.2 Fourier-transform infrared spectroscopy (FTIR)	133
4.2.3.3 Ultraviolet-visible spectroscopy (UV–vis)	133
4.2.4 Theoretical studies	135
4.2.4.1 Molecular modeling	135
4.2.4.2 Molecular dynamic simulation (MDS)	140
4.2.5 Mechanism of corrosion and inhibition	142
4.2.6 Conclusion	143
4.3 Quinoline Carbonitriles as Novel Inhibitors for N80 Steel Corrosion in Oil-Well Acidizing	145
4.3.1 Gravimetric Studies	147
4.3.1.1 Influence of inhibitor concentration	147
4.3.1.2 Temperature effects on the adsorption behavior of inhibitors	148
4.3.1.3 Adsorption isotherm	149
4.3.2 Electrochemical studies	150
4.3.2.1 Electrochemical impedance spectroscopy	150
4.3.2.2 Potentiodynamic polarization studies	154
4.3.3 Surface Analytical Measurements	157
4.3.3.1 Scanning electron microscopy (SEM)	157
4.3.3.2 FTIR measurements	158
4.3.4 Theoretical study	159
4.3.4.1 Computational Studies	159

4.3.5 Inhibition Mechanism	166
4.3.6 Conclusions	168
4.4 (E)-2-styryl-1H-benzo[d]imidazole as novel green corrosion inhibitor for carbon steel	170
4.4.1 Weight loss measurements	172
4.4.1.1 Influence of STBim concentration	172
4.4.1.2 Influence of temperature	173
4.4.1.3 Adsorption considerations	174
4.4.2 Electrochemical investigations	176
4.4.2.1 Impedance analyses	176
4.4.2.2 Frequency modulations	182
4.4.2.3 Polarization studies	185
4.4.3 Surface studies	187
4.4.3.1 Atomic force microscopy	187
4.4.3.2 FTIR studies	188
4.4.4 Theoretical studies	189
4.4.4.1 DFT simulations	189
4.4.5 Mechanism of corrosion inhibition	199
4.4.6 Conclusions	201
Chapter 5: Summary and Conclusions	
5.1 Summary	203
5.1.1 Substituted Triazines (TZs) as Corrosion Inhibitors	205
5.1.2 Chromeno Naphthyridines (CMs) as Corrosion Inhibitors	206
5.1.3 Quinolines (QDs) as Corrosion Inhibitors	207
5.1.4 Benzimidazole based corrosion inhibitors	208
5.2 Conclusions	209
5.3 Scope for future work	210
References.	211-230
List of publications.	231-232

LIST OF FIGURES AND SCHEMES

Figures		Page No.
Figure1.1	Corrosion process	2
Figure1.2	Formation of rust	10
Figure1.3	Uniform corrosion.	13
Figure 1.4	Galvanic corrosion.	13
Figure1.5	Crevice corrosion.	13
Figure 1.6	Pitting corrosion	13
Figure 1.7	Selective leaching	13
Figure 1.8	Intergranular corrosion	13
Figure 1.9	Stress corrosion	13
Figure 1.10	Erosion corrosion	13
Figure 1.11	Hydrogen damage	13
Figure 1.12	Evans diagram	30
Figure 1.13	(a) Anodic control (b) cathodic control, (c) mixed control.	31
Figure 1.14	A mixed potential plot for bimetallic couple of iron and zinc	32
Figure 1.15	Extrapolated Tafel curves	33
Figure 1.16	Hypothetical linear polarization plot	35
Figure 1.17	A general impedance measurements curve	37
Figure 3.1	FTIR spectra of synthesized Triazine derivatives	76
Figure 3.2	¹ H-NMR spectra of synthesized Triazine derivatives.	76
Figure 3.3	¹³ C-NMR spectra of synthesized Triazine derivatives	77
Figure 3.4	FTIR spectra of Naphthyridine derivatives.	80
Figure 3.5	¹ H NMR spectra of Naphthyridine derivatives.	81
Figure 3.6	Block diagram of impedance set up including constant phase element.	92
Figure 4.1	Structure of inhibitors: TZ-1, TZ-2 and TZ-3	99
Figure 4.2	Variation of inhibition efficiency ($\eta\%$) and corrosion rate (v_{corr})	100
Figure 4.3	Langmuir isotherm plot for the adsorption of TZs on N80 steel surface in 15% HCl	102
Figure 4.4	Nyquist plot for mild steel in 1 mol L-1 HCl without and with different Concentrations of TZs. (a) TZ-1 (b) TZ-2 (c) TZ-3	104
Figure 4.5	Bode (f vs $ Z $) and phase angle (f vs $\alpha\omega$) plot for N80 steel in 15% HCl Without and with different concentrations of TZs	105
Figure 4.5 (a)	Equivalent circuit	105
Figure 4.6	Potentiodynamic polarization curves for N80 in the absence and presence of different concentrations of TZs 350C (A) TZ-1, (B) TZ-2, (C) TZ-3	109
Figure 4.7	UV-visible spectra. (A) TZ-1, (B) TZ-2, (C) TZ-3	112
Figure 4.8	FTIR spectra of the inhibitors (K) TZ-1 (B) TZ-2, (C) TZ-3, FTIR Spectra of adsorbed inhibitor molecules on the N80 steel surface (L), (A) TZ-1, (B) TZ-2, (C) TZ-3	113
Figure 4.9	Three dimension AFM images and corresponding height profile diagram of N80 steel: (A, E) without TZs, (B, F) with TZ- 2, (C, G) TZ-1 (D, H) with TZ-3	115

Figure 4.10	Structure of inhibitors: CN-1, CN-2, and CN-3	120
Figure 4.11	Variation of inhibition efficiency ($\eta\%$) and corrosion rate (v_{corr})	121
Figure 4.12	Langmuir isotherm plot for the adsorption of CNs on N80 steel surface in 15% HCl	122
Figure 4.13	Fitted Nyquist plot for N80 steel in 15% HCl without and with different concentrations of CNs at 35 °C (a) CN-1 (b) CN-2 (c) CN-3. d,e: Equivalent circuit used. Bode (f vs $ Z $) and phase angle (f vs ω) plots for N80 steel in 15% HCl without and with different concentrations of CNs 35 °C (f) CN-1 (g) CN-2 (h) CN-3	124-125
Figure 4.14	Potentiodynamic Polarization curves for N80 in the absence and presence of different concentrations of CNs in 15% HCl at 35 °C (a) CN-1 (b) CN-2 (c) CN-3	130
Figure 4.15	Three dimension AFM images and corresponding height profile diagram of N80 steel: (a, e) without CNs, (b, f) with CN-1 (c, g) CN-2 (d, h) with CN-3	132
Figure 4.16	FTIR spectra of adsorbed CNs molecules on the N80 steel surface	133
Figure 4.17	UV-visible spectra for N80 in the absence and presence of optimum Concentrations of CNs in 15% HCl at 35 °C.	135
Figure 4.18	Optimized structures and, HOMO/ LUMO orbital density distribution for both neutral and protonated forms of CNs along with the orbital energy.	138
Figure 4.19	(a) Side and top views of the final adsorption of neutral forms of CNs on Fe (110) surface. (b) Side and top views of the final adsorption of protonated forms of CNs on Fe (110) surface	141
Figure 4.20	Inhibition mechanism of CNs adsorption on N80 steel surface	143
Figure 4.21	Structure of inhibitors: AHQ-1, AHQ-2, AHQ-3	147
Figure 4.22	(a) Effect of variation in the concentration of the quinoline derivatives on The corrosion inhibition efficiency at 308 K. (b) Effect of variation in solution temperature on the inhibition efficiency at 300 mg L ⁻¹ dose of inhibitors.	149
Figure 4.23	Plots of Langmuir isotherm for the adsorption of the three inhibitors On N80 steel surface in 15% HCl	150
Figure 4.24	Experimental and simulated Nyquist plots for the adsorption of the three quinoline derivatives on N80 steel surface in 15% HCl	153
Figure 4.25	Potentiodynamic polarization curves recorded for the adsorption of The three quinoline derivatives on N80 steel surface in 15% HCl	156
Figure 4.26	SEM images of the N80 steel surface after immersion for 24 h in 15% HCl In the absence of corrosion inhibitor (a), and in the presence of 300 mg L ⁻¹ Concentration of AHQ-1 (b), AHQ-2 (c), and AHQ-3 (d)	158
Figure 4.27	(a) FTIR spectra of the three quinoline derivatives;	159

	(b) FTIR spectra of the 161 quinoline derivatives recorded on the N80 steel surface following an immersion period of 24 h.	
Figure 4.28	Calculated pK_a values of the three quinoline derivatives.	160
Figure 4.29	Optimized molecular structures and the molecular orbital electron density distributions of the three quinolines in the neutral and protonated (*) form	162
Figure 4.30	Side (a, b) and corresponding top (c, d) views of the most stable configurations for the adsorption of AHQ-3 neutral and protonated on Fe (110) surface	165
Figure 4.31	Mechanism of adsorption and inhibition	168
Figure 4.32	(a) Variation of inhibition efficiency with concentration of STBim obtained from the weight loss measurements; (b) Variation of the inhibition efficiency with temperature; (c) Arrhenius plots for steel surface without and with inhibitor; (d) Langmuir isotherm plot for the adsorption of STBim on the steel surface.	176
Figure 4.33	Open circuit potential vs. time curves for carbon steel surface in 15% HCl without and with varying concentrations of STBim.	177
Figure 4.34	(a) Nyquist; (b) Bode, and phase angle plots for the adsorption of STBim on the carbon steel surface in 15% HCl. Fitted (c) Nyquist; (d) Bode, phase angle plots obtained for carbon steel in the absence and the presence of STBim in 15% HCl. Equivalent circuit models used to fit the EIS data obtained for the (e) blank and (f) inhibited steel samples	181
Figure 4.35	Intermodulation spectra obtained from the EFM measurements for the carbon steel immersed in 15% HCl solution in the absence and the presence of different concentrations of STBim.	183
Figure 4.36	Potentiodynamic polarization curves obtained for the carbon steel immersed in 15% HCl solution in the absence and the presence of different concentrations of STBim	186
Figure 4.37	Fe-slab and (E)-2-styryl-1H-benzo[d]imidazole (STBim) models used in our DFT simulation. a) An overview of the Fe-slab and the adsorbate with 25 Å vacuum to ensure that there is no interaction between the slab and its image along C-lattice constant. b) The optimized structures of STBim+ on Fe-slab, Color code, C: brown, N: blue, and H: white	188
Figure 4.38	FTIR spectra of the (c) pure STBim (d) STBim adsorbed carbon steel surface after immersion in 15% HCl	189
Figure 4.39	Fe-slab and (E)-2-styryl-1H-benzo[d]imidazole (STBim) models used in our DFT simulation. a) An overview of the Fe-slab and the adsorbate with 25 Å vacuum to ensure that there is no interaction between the slab and its image along C-lattice constant. b) The optimized structures of STBim+ on Fe-slab, c) Fe-slab + STBim-I, and d) Fe-slab + STBim-II	191

Figure 4.40	complexes. Color code, C: brown, N: blue, and H: white The binding charge densities of STBim ⁺ , and STBim on Fe-slab (100) analysis are shown, they are calculated following Eq. (3), we have subtracted the electron densities of the isolated slab and molecule from the total electron density of the complex. This analysis showing the interaction sites between the molecule and the slab. a), and c) the binding density of STBim ⁺ side and top view. b), and d) is the binding charge density of STBim on Fe-slab, side and top view. e), and f) are zoom in images of STBim ⁺ and STBim on Fe-slab showing only the accumulation of the electronic density (yellow), respectively. The iso surfaces is represented in a resolution of 0.005 electron/Å ³ . Yellow is rich and light-blue is depletion of the electron density. Fe-slab is represented by brown spheres, STBim is represented in balls and sticks. Color code, C: brown, N: blue, and H: white.	192
Figure 4.41	The protonated STBim ⁺ adsorbed on the iron slab with numbering of the heavy atoms to show the Fe-C bond distances reported in Table 4.15	193
Figure 4.42	show iron Fe-slab and adsorbed inhibitors colored by the atomic charges calculated using AIM approach, a color scale from 0.5 to -1.0e is shown. A clean iron slab is shown in two different views a): top view b) side view c) and d) show the adsorbed STBim ⁺ , and STBim-I on Fe-slab, respectively. Adsorbates are shown in sticks and metal surface are shown spheres	195
Figure 4.43	The planar average of the electrostatic potential along Z-axis for the three form of STBim molecule adsorbed on Fe-slab and the clean slab.	196
Figure 4.43	The planar average of the electrostatic potential along Z-axis for the three form of STBim molecule adsorbed on Fe-slab and the clean slab.	198
Figure 5.1	Structures of substituted Triazine inhibitors.	206
Figure 5.2	Structure of Chromeno Naphthyridines.	207
Figure 5.3	Structures of Quinoline derivative.	208
Figure 5.4	Structure of Imidazole derivative	209

List of Schemes

Scheme 3.1	Synthesis of Substituted Triazines.	75
Scheme 3.2	Synthesis of Chromeno naphthyridines.	80
Scheme 3.3	Synthesis of Hydroxyquinoline derivatives.	83
Scheme 3.4	Synthesis of substituted benzimidazole.	85

LIST OF TABLES		Page No
Table 3.1	Composition of N80 steel (wt. %).	71
Table 3.2	Composition of mild steel (wt. %)	72
Table 3.3	Name, Molecular formula, and Purity of Chemicals used.	74
Table 3.4	The name, structure and characterization data of Substituted Triazines based inhibitors.	78
Table 3.5	The name, structure and characterization data of Naphthyridine derivatives inhibitors	82
Table 3.6	The name, structure and characterization data of Hydroxy quinoline derivatives inhibitors	84
Table 3.7	The name, structure and characterization data of benzimidazole based inhibitors	86
Table 4.1	Calculated values of various isotherms for N80 steel in 15% HCl at the optimum concentration (800 mg/L) of TZs.	101
Table 4.2	Thermodynamic parameters for the adsorption of TZs on N80 steel in 15%HCl	102
Table 4.3	Electrochemical impedance parameters of N80 steel in 15% HCl at different concentrations of TZs at 308 K	107
Table 4.4	Electrochemical polarization parameters in the absence and presence of different concentrations of triazine derivative at 308 K.	111
Table 4.5	Electrochemical impedance parameters of N80 steel in 15% HCl at different concentrations of CNs at 35 °C.	127
Table 4.6	Potentiodynamic polarization parameters of N80 steel in 15% HCl at different concentrations of CNs at 35 °C.	129
Table 4.7	Energy order of the frontier molecular orbitals of CNs.	137
Table 4.8	Electrochemical impedance parameters of N80 steel in 15% HCl at different concentrations of AHQs at 308 K.	154
Table 4.9	Electrochemical polarization parameters of N80 steel in 15% HCl at different concentrations of AHQs at 308 K.	157
Table 4.10	Calculated quantum chemical parameters of quinoline derivatives in the neutral form.	161
Table 4.11	Adsorption parameters of AHQ-3 neutral and protonated as evaluated from the Monte Carlo simulations (all energy values in kcal mol ⁻¹)	163
Table 4.12	Electrochemical impedance parameters for carbon steel sample in 15% HCl at different concentrations of STBim.	182
Table 4.13	Electrochemical EFM parameters obtained for carbon steel sample in 15% HCl without and with different concentrations of STBim.	184
Table 4.14	Potentiodynamic polarization parameters for carbon steel in 15% HCl obtained at different concentrations of STBim.	186
Table 4.15	The optimized Fe-C bond distances between the adsorbate and slab for STBim+ and STBim-I. Carbon and Nitrogen numbering is following scheme shown in Figure 4.43	194

Abbreviations used

$IE\%$ =Percentage of inhibition efficiency

C_R =Corrosion rate ($\text{mgcm}^{-2}\text{h}^{-1}$)

C_R^0 =Corrosion rate in uninhibited system ($\text{mgcm}^{-2}\text{h}^{-1}$)

C_R^i = Corrosion rate in inhibited system ($\text{mgcm}^{-2}\text{h}^{-1}$)

Y^0 =amplitude of the CPE ($\text{s}^n\Omega^{-1}\text{cm}^{-2}$)

j = imaginary unit ($\sqrt{-1}$)

ω =angular frequency ($2\pi f$, f the frequency)

f = Frequency of component of impedance (s^{-1})

C_{dl} =Double layer capacitance ($\mu\text{F cm}^{-2}$)

C_f =film capacitance

C =capacitance

R_s =Solution resistance(Ωcm^2)

R_L =Inductance resistance (Ωcm^2)

R_{ct} =charge transfer resistance in absence of inhibitor(Ωcm^2)

R_p =polarization resistance (Ωcm^2)

i_{corr}^0 =Corrosion current density in uninhibited solution

$(\mu\text{Acm}^{-2})i_{\text{corr}}^i$ = Corrosion current density in inhibited solution (μA

$\text{cm}^{-2})E_{\text{corr}}$ =Corrosion potential (mV/SCE)

β_a =Anodic Tafel constant (mV dec^{-1})

β_c =Cathodic Tafel constant (mV dec^{-1})

A =Arrhenius pre-exponential factor ($\text{mgcm}^{-2} \text{h}^{-1}$)

E_a =Activation energy(kJmol^{-1})

R =Universal gas constant ($\text{JK}^{-1}\text{mol}^{-1}$)

T =Absolute temperature (K)

N =Avogadro's number ($6.023 \times 10^{23}\text{mol}^{-1}$)

h =Planck's constant (J-s)

K_{ads} =Adsorption equilibrium constant (Lmol^{-1})

$\Delta G^\circ_{\text{ads}}$ =Gibbs freeenergy of adsorption(kJmol^{-1})

θ =Degree of surface coverage of metal

C_{inh} =Concentration of inhibitor (molL^{-1} ,ppm)

E_{HOMO} =Energy of highest occupied molecular orbital

E_{LUMO} =Energy of lowest unoccupied molecular orbital

ΔE =Energygap between HOMO and LUMO

χ_{Fe} =Electro negativity of iron

χ_{inh} =Electronegativity of inhibitor

σ = softness

η_{Fe} =Hardness of iron

η_{inh} =Hardness of inhibitor

Φ =work function

ΔN =Fraction of electron transfer

E_{molecule} =Energy of the inhibitor molecule before adsorption of inhibitor molecules

$E_{\text{interaction}}$ = Interaction energy between metal surface and inhibitor molecules

PREFACE

Corrosion is a gradual destruction of materials (usually metals) by chemical and/or electrochemical reaction with their environment. Corrosion causes numerous failures and enormous losses in a number of industries. Failures resulting from inability of metal to support the designed load requirement due to loss of metal caused by corrosion effect can be controlled economically using the chemical inhibitors. Besides the effectiveness, most of the chemical inhibitors are associated with toxicity, disposal and enormous cost. The present research work has been focused on Synthesis of Heterocyclic compounds as acidizing corrosion inhibitors for carbon steel in 15% hydrochloric acid. The thesis is divided into five chapters.

Chapter 1 deals with the introduction of corrosion, highlighting the definition of corrosion, Economic importance of corrosion, Different form of corrosion, Methods of Corrosion Control, theory and mechanism of corrosion principles. Aim and objectives of the research have been elaborated.

Chapter 2 focuses on the literature survey relevant to corrosion of carbon steel (N-80 Steel and mild steel) in the acid environment, along with the general introduction of corrosion inhibitors: definition, types and mechanism. Chapter 3 deals with the materials and methods details including materials, synthesis of organic inhibitors, sample preparation, chemicals and methods adopted such weight loss, electrochemical impedance spectroscopy (EIS), potentiodynamic polarization (PDP), surface analysis (SEM/EDX/AFM /FTIR) and computational simulations.

(quantum chemical calculations and molecular dynamic) for the evaluation of corrosion inhibition property have been described.

Chapter 4 deals with the results and discussion on corrosion inhibition of N-80 steel and mild steel in 15% hydrochloric acid by four series of inhibitors: Substituted Triazines (TZs) derivatives (Series I), Chromeno Naphthyridines (CNs) derivatives (Series II), Quinolines (AHQs) (Series III) and Benzimidazole based corrosion inhibitors (Series IV) using weight loss (WL), electrochemical impedance spectroscopy (EIS) and potentiodynamic polarization (PDP). The inhibited and uninhibited metal surface was characterized using the scanning electron microscopy (SEM), energy dispersive X-ray spectroscopy (EDX), atomic force microscopy (AFM), Fourier-transform infrared Spectroscopy-Attenuated total reflection- (FTIR-ATR) and UV-vis spectroscopy. The theoretical studies: quantum chemical calculation and molecular dynamics simulation were used to obtain insights in the inhibition mechanism of the inhibitor molecules on the metal surface.

A plausible mechanism of corrosion inhibition has been proposed on the basis of experimentally and theoretically obtained results.

Chapter 5 provides general summary, conclusions and suggests future work.